Available online at www.sciencedirect.com
ScienceDirect
Nuclear Instruments and Methods in Physics Research A 583 (2007) 42–48
NUCLEAR INSTRUMENTS & METHODS IN PHYSICS RESEARCH Section A
www.elsevier.com/locate/nima

Charge amplitude distribution of the Gossip gaseous pixel detector

V.M. Blanco Carballo[a], M. Chefdeville[b], P. Colas[c], Y. Giomataris[c], H. van der Graaf[b], V. Gromov[b], F. Hartjes[b,*], R. Kluit[b], E. Koffeman[b], C. Salm[a], J. Schmitz[a], S.M. Smits[a], J. Timmermans[b], J.L. Visschers[b]

[a] *Twente University, Enschede, The Netherlands*
[b] *NIKHEF, P.B. 41882, 1009DB Amsterdam, The Netherlands*
[c] *Saclay, Gif-sur-Yvette, France*

Available online 31 August 2007

Abstract

The Gossip gaseous pixel detector is being developed for the detection of charged particles in extreme high radiation environments as foreseen close to the interaction point of the proposed super LHC. The detecting medium is a thin layer of gas. Because of the low density of this medium, only a few primary electron/ion pairs are created by the traversing particle. To get a detectable signal, the electrons drift towards a perforated metal foil (Micromegas) whereafter they are multiplied in a gas avalanche to provide a detectable signal. The gas avalanche occurs in the high field between the Micromegas and the pixel readout chip (ROC). Compared to a silicon pixel detector, Gossip features a low material budget and a low cooling power. An experiment using X-rays has indicated a possible high radiation tolerance exceeding 10^{16} hadrons/cm^2.

The amplified charge signal has a broad amplitude distribution due to the limited statistics of the primary ionization and the statistical variation of the gas amplification. Therefore, some degree of inefficiency is inevitable. This study presents experimental results on the charge amplitude distribution for CO_2/DME (dimethyl-ether) and Ar/iC_4H_{10} mixtures. The measured curves were fitted with the outcome of a theoretical model. In the model, the physical Landau distribution is approximated by a Poisson distribution that is convoluted with the variation of the gas gain and the electronic noise. The value for the fraction of pedestal events is used for a direct calculation of the cluster density. For some gases, the measured cluster density is considerably lower than given in literature.

PACS: 29.40.Cs

Keywords: Micromegas; Gaseous detector; Cluster density; Charge signal distribution

1. Introduction

Basically, the tracking of Gossip occurs by measuring the locus of the individual electrons that are liberated by the interaction of a charged particle with a thin layer of gas. Occasionally, this electron has sufficient energy to create a number of secondary electron/ion pairs in the gas. Mostly, the range of the excited electron is of the order of a few micrometers, but incidentally electrons with a millimeter range (δ-electrons) may occur as well. Since the number of electron–ion pairs is generally small, amplification by a gas avalanche is required to obtain a detectable signal. For Gossip, the avalanche is formed in the strong electrical field (~10 kV/mm) between a perforated metal foil (Micromegas) and a pixel chip.

Fig. 1 illustrates the basic operation of Gossip. An ionization electron, which is created in the gap between the conducting cathode foil and the Micromegas, drifts towards the Micromegas and is subsequently collected by one of the Micromegas holes. Hereafter, it initiates an avalanche in the high but constant field between the Micromegas and the readout chip (ROC). Amplification factors up to 10,000 can be obtained in this way. The pitch of the holes of Micromegas may be as small as 50 μm, enabling a fine granularity pixel detector. The gas

*Corresponding author. Tel.: +31 20 5925010; fax: +31 20 5925155.
E-mail address: F.Hartjes@nikhef.nl (F. Hartjes).

0168-9002/$ - see front matter
doi:10.1016/j.nima.2007.08.199

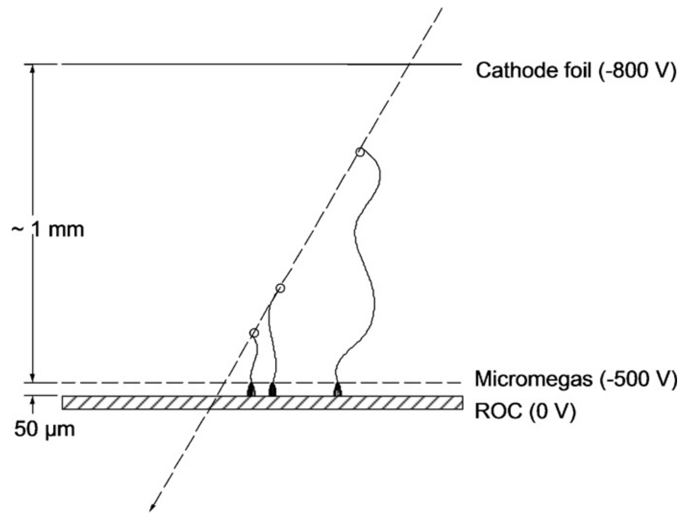

Fig. 1. Principle of Gossip.

amplification with Micromegas shows a strong exponential dependence on the applied voltage. But in contrast to this, the gas amplification does not depend much on the width of the amplification gap if the width is of the order of 50 μm [1,2].

The collection time of the charge signal is determined by several parameters. In the high field of the amplification gap, electrons have a drift velocity exceeding 50 μm/ns [3], so their collection time may be neglected. But also for the ions, it takes a relatively short time (about 50 ns for Argon [4]) to traverse the full gap width. So taking into account the transition time of 20 ns maximum of the primary electrons across the 1 mm wide drift gap, we obtain a total charge collection time of around 60 ns. The position resolution is expected to be comparable to that of a silicon sensor. Note that unlike other gaseous detectors, the effect from δ-electrons is expected to be minimal since the primary electrons are reconstructed individually in space and time by the pixel electronics.

Drawback of using a separated Micromegas foil is the critical mechanical assembly. In addition, it suffers from a few percents of inactive area at the supporting pillars. Although the ionization electrons that are generated in the drift space above a pillar are still collected, they will be focused to adjacent pixel cells causing deterioration of the position resolution. Therefore, a more practical solution for mass production has been devised with InGrid where the width of the amplification gap and the alignment of the Micromegas holes to the pads of the ROC are better guaranteed. At the InGrid concept a Micromegas foil is created directly onto the chip by wafer post-processing [2,5]. This foil is fixed on the ROC surface by pillars of SU8 photo resist. The pillars are very narrow and are easily hidden between the holes eliminating the dead area. Charge signal spectra of X-rays from an ^{55}Fe source measured with InGrid show a spectrum with a high resolution compared to other gaseous detectors [2]. Recently also, structures with two and three piled-up Micromegas foils have been produced in the same way.

Compared to a silicon pixel sensor, the advantages of Gossip are the complete absence of bias current and a very low input capacity (~15 fF). There are no hard limits on the operating temperature; a practical range is between −30 and 50 °C. To profit from the low input capacity and low bias current, for Gossip a dedicated low-power pixel chip is being developed in 130 nm technology. The preamp chip Gossipo-1 features power consumption less than 2 μW per pixel cell at a shaping time of 40 ns [6]. This opens the way for lower power consumption at a smaller pitch compared to silicon tracking sensors. In addition, the more relaxed temperature control and the absence of heat from the detector medium enable a greatly simplified and lighter cooling system. The material budget of the sensor alone is very small ($<0.1\%$ X/X_0) because of the absence of bump bonds and a low-density detector medium while also the reduced cooling requirements significantly diminish the material of the whole tracker system. An ageing test done with an X-ray source [7] indicates a permissible charged hadron dose exceeding $10^{16}\,\mathrm{cm}^{-2}$ at a gas amplification of 1000. This result is in agreement with previous observations [8].

A disadvantage of the Gossip technology compared to a solid-state detector is the requirement of an additional high-voltage supply for the Micromegas with a critical adjustment. A voltage increase of 4% resulted in an increase of the average charge amplitude by a factor of 2 for the measurements presented here. However, a lesser dependence may be expected on the atmospheric pressure and the temperature [1,2]. Gaseous detectors have a general tendency for sparking that cannot be avoided. Experience has shown that these discharges easily destroy the pixel chip. Investigations are going on now to overcome this problem, e.g. to limit the peak discharge current by covering the pixel chip with a resistive layer of amorphous silicon.

2. Thickness of the gas gap and cluster density

It is clear that for tracking at the super LHC, the thickness of the gas layer should be reduced to the minimum to avoid ballistic deficit and to get the highest possible rate capability. On the other hand, the finite amount of ionization clusters that are created along the track of a minimum ionizing particle sets a minimum to the thickness of the gas gap. The cluster density is dependent on the applied counter gas but a value of $30\,\mathrm{cm}^{-1}$ at atmospheric pressure is well possible. This sets the lower limit on the width of the gas gap to about 1 mm to obtain an efficiency of 95% for a perpendicular incidence.

We assume that the ionization clusters are Poisson-distributed along the track. Accordingly, the chance $P(n)$ on having n clusters across the drift gap is given by

$$P(n) = -\frac{\lambda^n}{n!}\,\mathrm{e}^{-\lambda} \quad (1)$$

where λ is the expected number of clusters in the drift gap. Expression (1) alone in principle would result into a distribution spectrum of δ functions, in practice, a continuum is formed because of the variation of the gas amplification.

For single electron events, several investigators [9–11] have shown that for gas amplifications larger than 100, the distribution function of the gas amplification is given by a simple exponential decay starting at zero. For this, it is assumed that the ionization probability of the electron depends only on the electric field and not on its history. This assumption is fulfilled in a weak uniform amplification field. But for strong non-uniform electric fields with high ionization probability, Alkhazov [12] has explained, based on the ideas of Legler [13], that the distribution of the gas amplification of a single electron is better described by the Pólya distribution

$$P(x) = -\frac{m^m}{\Gamma(m)}\, x^{m-1}\, \mathrm{e}^{-mx} \tag{2}$$

where x is the value of the resulting charge signal and m is the Pólya distribution factor (pdf), m being a positive number $\geqslant 1$ with a value depending on the applied counter gas, the electric field in the amplification region and the geometry.

For n primary electrons, there exists an explicit expression for integer values of m of the distribution function by integrating Eq. (2). Accordingly, we obtain

$$P(x,n) = \frac{x^{n-1}}{(n-1)!}\, \mathrm{e}^{-x} \quad \text{for } m = 1 \tag{3}$$

and

$$P(x,n) = \frac{2^{2n}}{(2n-1)!}\, x^{2n-1}\, \mathrm{e}^{-2x} \quad \text{for } m = 2. \tag{4}$$

In practice, we have to take into account the electronic noise as well. For this we assume a Gaussian distribution that is independent of the magnitude of the charge signal:

$$P(x) = \frac{1}{\sigma\sqrt{2\pi}}\, \mathrm{e}^{-x^2/2} \tag{5}$$

where σ is the width of the Gaussian distribution. The example in Fig. 2 depicts the Poisson distribution (spikes) for an average number of six primary electrons and a gas gain of 2000. The Poisson distribution is convoluted with the Pólya distribution (4) for $m = 2$ and with the Gaussian noise (5) of $\sigma = 500$ electrons. In addition, 1.9% pedestal events have been added as a simulation of the background count rate of the experimental set-up. The convoluted curve is smooth with the exception of the pedestal peak which is not broadened by the Pólya function.

For an experimental set-up with an external scintillator trigger, expression (1) opens the way to derive the cluster density d_{cl} from the measured inefficiency $P(0)$ according to

$$d_{\mathrm{cl}} = -\frac{\ln[P(0)]}{D} \tag{6}$$

where D is the width of the gas gap. However, when trying to fit the convoluted Poisson function with the experimental curve, a clear discrepancy can be expected since the primary ionization in gaseous medium is better described by a Landau distribution where plural electron clusters are considered. But on the other hand, for most gases, at least 90% of the clusters contain only one electron as is shown by the simulation program HEED [14]. Therefore, the small charge signals in the pedestal peak region may be assumed to consist of almost exclusively single electron clusters, so the Poisson distribution gives a fairly good description here, while a clear disagreement is expected at the tail of the distribution. Note that for the application of

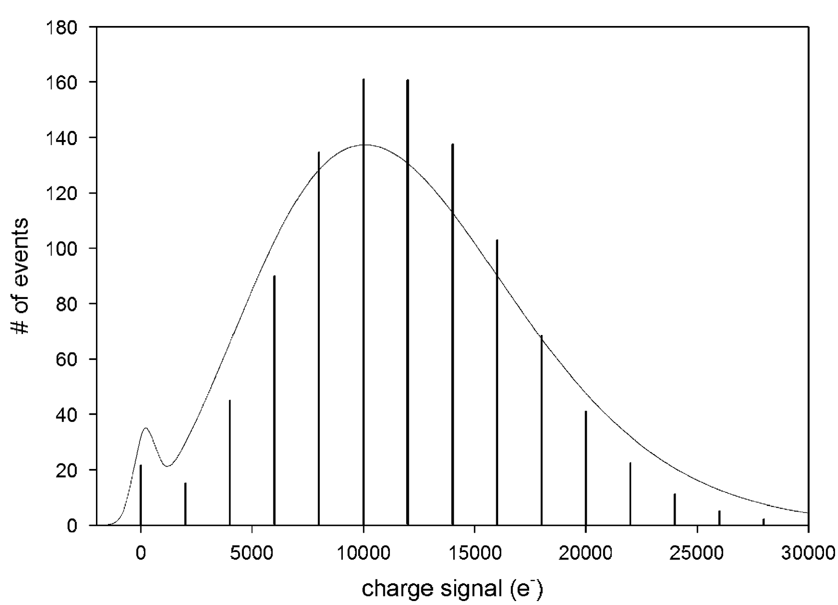

Fig. 2. Example of the convolution of a Poisson distribution with a Pólya distribution and the Gaussian electronic noise.

Gossip as a tracking detector using binary output, the tail is hardly relevant.

3. Experimental set-up

The charge signal spectra were measured using the NIKHEF characterization station [15]. In this device, the β-rays of an 18.5 MBq (50 μCi) ^{90}Sr source pass a collimator consisting of a plastic base that is covered by a tungsten cap. In this way, a pencil beam with $\sigma = 0.2$ mm is obtained. Subsequently the β's pass the Gossip prototype and finally hit a small scintillator (Fig. 3). The charge signal of Gossip is fed into an Amptek A250 charge-integrating amplifier and subsequently shaped by two A275 shapers to a 2 μs wide pulse. In addition, the baseline of the signal is stabilized by an Amptek BLR1 baseline restorer. The trigger was provided by a small scintillator (3 × 3 mm) that was coupled by a light guide to a Hamamatsu H5783 photomultiplier. Without excitation by the source, a dark count rate of only 0.025 Hz was measured, probably mainly from cosmics. But with the 18.5 MBq ^{90}Sr source, the dark count rate of the scintillator increased to 0.24 Hz, probably from Bremsstrahlung triggers. Because of the very low operating current and the high local fields on the Gossip detector, the characterization station had to be permanently flushed with dry air to avoid surface currents.

The triggered data acquisition used a National Instruments PCI-6024E DAQ board housed in a PC. The DAQ board also controlled the Micromegas voltage with a resolution of 0.5 V and monitored the Micromegas current with a resolution of 2.5 pA. A software trip was set on 5 nA.

The Gossip prototype (Fig. 4) consisted of a 523 μm thick silicon carrier as a dummy ROC that was covered with a 15 × 15 mm wide thin film aluminium electrode. Onto this, a 3 μm thick high resistivity amorphous silicon layer (SiProt) was deposited for spark-protection experiments. Most likely, the presence of this layer did not play a role for the measurements that are presented here.

Onto the silicon carrier, a 3 μm thick Micromegas foil was attached having 35 μm wide holes with a pitch of $60 \times 60\ \mu m^2$ and supported by 50 μm high pillars. On the Micromegas foil, a 1.2 mm high frame from Torlon was glued that was covered by a cathode foil from coppered Kapton. As a glue, Araldite was used. The gas was flushed via two thin Peek tubes of 1/32″ outer diameter. In this way, a gastight chamber was created with a volume of only 0.2 ml.

A drawback of using a very wide electrode was the high capacity (48 pF) to the Micromegas foil. In combination with noise pickup from external sources, this led to a noise level of the order of 1200e$^-$. Therefore, high gas

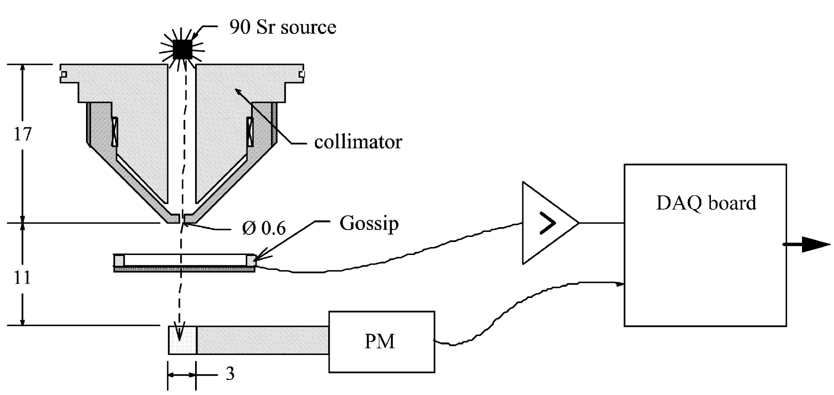

Fig. 3. Principle of the NIKHEF characterization station (dimensions in mm).

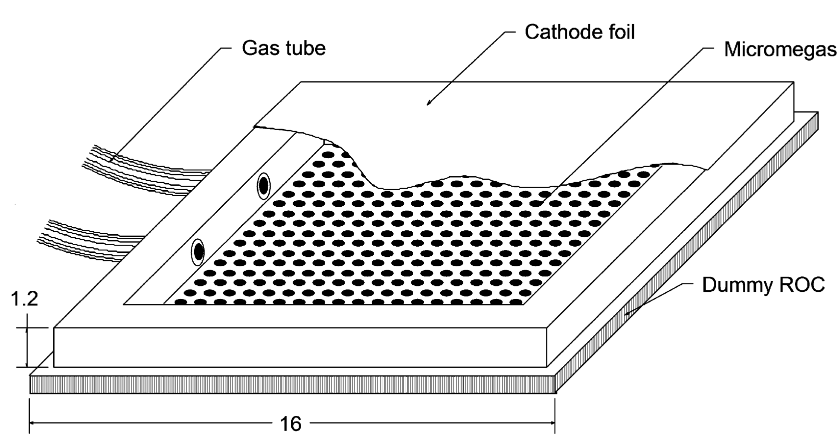

Fig. 4. Gossip prototype (dimensions in mm). The size and pitch of the Micromegas holes have been scaled 10 × for better visibility.

amplification (preferably 10–15k) was required to enable a proper analysis of the pedestal peak.

The electrode of the dummy ROC was AC-coupled to the preamp via a 10 nF capacitor and DC-coupled to ground via a 1.1 GΩ resistance. The filtered Micromegas voltage and cathode voltage were supplied via a 200 MΩ resistance. Using a passive electronics network, the cathode voltage was automatically set about 200 V more negative than the Micromegas voltage. To check for a possible loss of signal because of a too long drift time in the slow-gas mixture CO_2/DME (dimethyl-ether), a few spectra were measured with the double-voltage difference between cathode and Micromegas. No effect on the charge signal spectrum was observed.

Generally, the prototype Gossip detector was flushed with 2–3 ml/min, implying an exchange rate of 600–900 h^{-1}. The gas flow was regulated by mass flow controllers and calibrated using a soap bubble flow meter. The chamber was kept at an overpressure of 1 mbar.

4. Measurements and analysis

For the analysis presented here, in total 12 charge signal spectra were measured, six with CO_2/DME 46/54, two with DME alone, two with Ar/iC_4H_{10} 78/22 and two with Ar/iC_4H_{10} 50/50. For pure CO_2 and iC_4H_{10}, it was not possible to set the gas gain sufficiently high to enable a proper analysis of the pedestal peak. Most spectra were made with 50k events. However, because of the high gas gain that was required, sometimes the measurement was earlier terminated because of an over-current to the Micromegas. The Micromegas current was initially relatively high (of the order of 1 nA). But after a few days of more or less permanent high voltage on the Micromegas, the current was reduced to about 100 pA.

The measured distribution curve was fitted with the sum of the convoluted Poisson distribution and a Gaussian pedestal peak, by using the routine NEWANA-POISSON [15]. The convoluted Poisson distribution is calculated from the Poisson function (1) that is convoluted with the Pólya distribution function (3) or Eq. (4) and the Gaussian electronic noise (5). The Poisson value $P(0)$ is fixed at zero. The pedestal peak is a Gaussian centered at charge signal zero and having a preset width equal to the electronic noise. In total, the fitting routine uses three independent parameters: (1) the horizontal scaling factor of the convoluted Poisson which is proportional to the gas gain, (2) the surface of the convoluted Poisson and (3) the fraction of pedestal events.

For each spectrum, at first several fits were made with different values for the average number of clusters and using pdf = 2 until a close agreement to the rising edge of the measured distribution was obtained. For practical reasons in the analysis, we virtually modified the width of the gas gap to get a different number of clusters. The Landau tail was skipped from the data that were used for the fit since no agreement with the Poisson distribution can be expected there. As this is a bit arbitrarily recipe, the value for the horizontal scaling factor that was obtained in this way had a relatively large error. But on the other hand, the outcome of the analysis, i.e. the fraction of pedestal events, was constant for all tight fits in the pedestal region.

The measured value of the fraction of pedestal events was used to calculate the cluster density using expression (6). But note that basically the cluster density can also be independently deduced from the number of primary electrons that gave the best fit to the experimental curve. However, in general, the exact value of the pdf is not known in advance, so we used this method only to verify the cluster density that was obtained from the pedestal measurement.

Before calculating the cluster density from the pedestal fraction, we first have to subtract the background of γ radiation that is hitting the scintillator (Bremsstrahlung). For a silicon sensor (ATLAS SCT baby sensor [16]) of 280 μm thickness, we measured $1.54 \pm 0.07\%$ pedestal events at a trigger rate of 17.5 Hz. But for the Gossip prototype using a 523 μm thick silicon substrate, we got a smaller trigger rate (9.0 Hz) and thus a higher number of background events. Assuming a constant background rate, we would therefore expect for the Gossip prototype a pedestal background of at least $2.99 \pm 0.14\%$. This level is confirmed by measurements with a gas mixture (Ar/iC_4H_{10} 50/50) that is expected to have a high cluster density according to literature (51.5 cm^{-1}) and thus would give a pedestal fraction of only 0.2% due to inefficiency. The measured pedestal was $3.01 \pm 0.05\%$ exactly matching the assumption. Obviously, there is no effect from possible additional Bremsstrahlung that might be created by the thicker silicon of the Gossip prototype. Note that, in general, a few percent of background pedestals make the fitting of the pedestal peak more reliable.

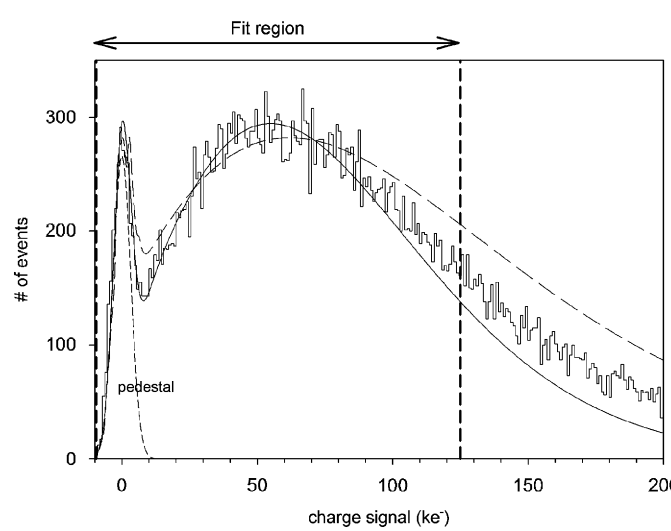

Fig. 5. Example of a charge signal spectrum. Two different fit curves of the convoluted Poisson are shown: (1) pdf = 2, drift gap = 1.1 mm (solid line) and (2) pdf = 1, drift gap = 1.2 mm (dashed line).

Table 1
Results of the cluster density measurements

Gas	Mixing ratio	Measured pedestal background (%)	Cluster density (this measurement) (cm^{-1})	Cluster density (from Smirnov expression) (cm^{-1})
DME/CO_2	54/46	1.98 ± 0.19	33.3 ± 0.8	49.9
DME	100	3.13 ± 0.30	29.4 ± 0.9	60.7
CO_2	100	–	37.9 ± 1.4[a]	37.2
Ar/iC_4H_{10}	78/22	3.4 ± 0.5	28.7 ± 1.3	34.8
Ar/iC_4H_{10}	50/50	0.2 (−0.2/+0.4)	>43	51.5

[a]The cluster density for CO_2 could not be measured directly but was derived from the measured cluster densities of the DME/CO_2 mixture and pure DME.

Fig. 5 shows an example of the measured charge signal spectrum from DME/CO_2 54/46 at $V_{\mathrm{Micromegas}} = -600\,\mathrm{V}$. For pdf = 2 and a gas gap width of 1.1 mm (solid line), we get a close fit to the rising edge of the experimental curve. But as expected, the (Poisson) tail of the fitted curve decays faster than the experimental distribution. As an example, the curve for pdf = 1 and a 1.2 mm wide gas gap is plotted as well. Although this last curve gives a poor agreement with the data, we can still get a good fit for pdf = 1 by increasing the average number of primary electrons. It appeared that at a gas gap width of 1.5 mm, we get in the pedestal region the same close fit for pdf = 1 as for pdf = 2 with a 1.1 mm gas gap, although expressions (2) and (3) are mathematically quite different.

In Table 1, the measured cluster density is compared with the result from a semi-empirical expression from literature [17]. Here, the cluster density n_D is given by

$$n_{\mathrm{D}} = \frac{Z_{\mathrm{m}}}{Z_{\mathrm{av}}^{0.4}} \tag{7}$$

where

$$Z_{\mathrm{av}} = \frac{\sum f(n_{\mathrm{a}}) \times Z(n_{\mathrm{a}})}{\sum f(n_{\mathrm{a}})} \tag{8}$$

is the mean nuclear charge of all atoms of the molecule, and Z_m is the summed charge of all nuclei of the molecule.

The results show a good agreement with literature for CO_2. But for DME, only half of the literature value [18] was measured while also the $Ar/i\text{-}C_4H_{10}$ mixture is 18% lower than expected. The difference with these measurements may be explained from the method that was used for the quoted measurements, i.e. electron counting at pressures in the millibar range where due to diffusion, clusters of more than one electron might be erroneously counted as more than one event.

Once the cluster density is known, we can also determine the correct pdf of the gas gain variation by interpolation between the values found for pdf = 1 and 2. For the measurement of Fig. 5 where a good fit was obtained with a gap thickness of 1.1 mm for pdf = 2 and 1.5 mm for pdf = 1, we obtain accordingly pdf = 1.8 for the actual gap width of 1.2 mm.

As an additional check, we tried to fit the charge distribution curve of pure DME using the value of the cluster density from literature ($60.7\,cm^{-1}$). But even for pdf = 1, the predicted curve was clearly too narrow.

5. Conclusions

The fraction of pedestal events of the charge signal distribution of an externally triggered detector can be used in a novel method to calculate the cluster density. The method is based on the assumption of a Poisson-like spatial distribution of the ionization clusters along the track. Compared to the values found in literature, the value measured for DME was surprisingly low while also an Ar/iC_4H_{10} mixture gave a lower value than expected.

Fitting the charge signal distribution with a Poisson-based function gives a good approximation for the rising edge of the distribution ignoring the Landau tail. This has the advantage of a simple-fitting routine based on explicit expressions. The low value for DME that was obtained from the pedestal was independently confirmed by the shape of the measured curve. Using the literature value, the convoluted Poisson curve could not be brought to agreement with the measured distribution.

References

[1] Y. Giomataris, Nucl. Instr. and Meth. A 419 (1998) 239.
[2] V.M. Blanco Carballo, C. Salm, J. Schmitz, S. Smits, M. Chefdeville, H. van der Graaf, J. Timmermans, J.L. Visschers, Nucl. Instr. and Meth. A 576 (2007) 1.
[3] A. Peisert, F. Sauli, Drift and diffusion of electrons in gases: a compilation (with an introduction to the use of computing programs), CERN Report CERN-84-08, 1984.
[4] W.L. Harries, J. Phys. D 1 (1) (1978) 1853.
[5] V.M. Blanco Carballo, et al., A miniaturized multiwire proportional chamber using CMOS wafer scale post-processing, Proceedings of ESSDERC 2006 Conference, 2006, p. 129.
[6] V. Gromov, R. Kluit, Prototype of the front-end circuit for the GOSSIP chip in the 0.13μm CMOS technology, CERN Yellow Report CERN 2007-001, 2007, p. 253.
[7] H. van der Graaf, et al., Nucl. Instr. and Meth. A (2007), in press, doi:10.1016/j.nima.2006.06.096.
[8] G. Puill, J. Derré, Y. Giomataris, P. Rebourgeard, IEEE Trans. Nucl. Sci. NS-46 (6) (1999) 1894.
[9] H.S. Snyder, Phys. Rev. 72 (1947) 181.
[10] R.A. Wijsman, Phys. Rev. 75 (1949) 833.
[11] W. Legler, Zeitschr. Phys. A Hadr. Nucl. 140 (2) (1955) 221.

[12] G.D. Alkhazov, Nucl. Instr. and Meth. 89 (1970) 155.
[13] W. Legler, Z. Naturforsch. 16a (1961) 253.
[14] Igor Smirnov, HEED, program to compute energy loss of fast particles in gases, version 1.01, CERN.
[15] F. Hartjes, Manual of the NIKHEF characterisation station, NIKHEF Internal Report NIKHEF 07–002, 2007.
[16] Gennaro Ruggiero, Signal generation in highly irradiated silicon microstrip detectors for the ATLAS experiment, Ph. D. Thesis, University of Glasgow, Glasgow, UK, 2003.
[17] I.B. Smirnov, Nucl. Instr. and Meth. A 554 (2005) 474.
[18] A. Pansky, G. Malamud, A. Breskin, R. Chechik, Nucl. Instr. and Meth. A 323 (1992) 294.